MNRAS **000**, 1–9 (2016) Preprint 27 October 2016 Compiled using MNRAS LATEX style file v3.0

The highly ionized, high velocity gas in NGC 6231

Derck Massa,[1]⋆
[1]*Space Science Institute, 4750 Walnut St., Suite 205, Boulder, Colorado 80301, USA*

Accepted XXX. Received YYY; in original form ZZZ

arXiv:1610.08130v1 [astro-ph.SR] 26 Oct 2016

ABSTRACT

It is well known that clusters of massive stars are influenced by the presence of strong winds, that they are sources of diffuse X-rays from shocked gas, and that this gas can be vented into the surrounding region or the halo through the champagne effect. However, the details of how these different environments interact and evolve are far from complete. This paper attributes the broad C IV$\lambda\lambda$1500 absorption features (extending to -1900 km s^{-1}) that are seen in the spectra of main sequence B stars in NGC 6231 to gas in the cluster environment and not the B stars themselves. It is shown that the presence of a WC star, WR 79, in the cluster makes this gas detectable because its wind enriches the cluster gas with carbon. Given the available data, it is not clear whether the absorbing gas is simply the far wind of WR 79 or a collective cluster wind enriched by carbon from the wind of WR 79. If it is simply due to the wind, then this wind must flow, unimpeded for more than 2 pc, suggesting that the inner region of the cluster is nearly devoid of obstructing material. If it is actually a collective wind from the cluster, then we could be witnessing an important stage of galactic feedback. In either case, the observations provide a unique and significant piece to the puzzle of how massive, open clusters evolve.

Key words: stars: winds, outflows – stars: Wolf-Rayet – ISM: H II regions – open clusters and associations: NGC 6231

1 INTRODUCTION

Wolf Rayet stars have powerful, highly ionized stellar winds, and the signature of these winds define their spectra class. Their winds have been imaged on scales of hundreds of AU (e.g., Tuthill et al. 2008) and their power is evident from the wind blown bubbles they can produce, which can be several pc in diameter (e.g., Cazzolato & Pineault 2000; Naze et al. 2003). In a cluster, these winds may carve out large cavities around the star or may interact with the winds of other cluster members. This paper shows that because WR 79 (HD 152270) resides in the young, compact open cluster NGC 6231, it is possible to use the main sequence B stars (BVs thereafter) in the cluster to probe the influence of its carbon rich, massive wind at distances more than a parsec from the star. This wind is identified as the source of strong, high speed C IV$\lambda\lambda$1550 absorption seen in *IUE* spectra of BVs in the core of NGC 6231. The following sections provide: an overview of NGC 6231 and WR 79, including why a previous explanation for the high speed absorption is no longer tenable (§ 2); an explanation of why the wind of WR 79 can be observed in NGC 6231 (§ 3); a derivation of the absorption profiles expected for BVs embedded in a wind (§ 4); fits of the model profiles to the 2 BVs in NGC 6231 that have high dispersion *IUE* spectra (§ 5), and; a discussion of the results (§ 6).

2 NGC 6231

NGC 6231 is a compact open cluster at the core of Sco OB1, at a distance of 1.64 kpc (Balona & Laney 1995). The core of the cluster contains numerous BVs, 10 O stars, a B supergiant and the WC+O star WR 79. Its stellar content has been well studied (e.g., Schild et al. 1969; Baume et al. 1999), and it is a site of ongoing star formation (Sana et al. 2007). Polarimetric observations by Feinstein et al. (2003) suggest there has been a supernova explosion in the cluster, but they noted that their observations are also consistent with an expanding bubble of the sort attributed to the WC stars WR 101 and WR 113 by Cappa et al. (2002). Red DSS2 images of the region show that NGC 6231 is within a large, $\sim 1.7^\circ \times 3.5^\circ$ (~ 50 pc $\times 100$ pc), cavity centered near ζ^1 Sco, and give the impression that the cluster might be venting gas from its H II region. However, such gas has not been detected. WR 79 is one of the most luminous objects in the cluster. It is a colliding wind binary system whose wind

⋆ E-mail: dmassa@spacescience.org

© 2016 The Authors

was modeled by Hill et al. (2000), who showed that the WC component dominates the overall wind flow.

Some years ago, Massa et al. (1984) noticed that the low dispersion *IUE* spectra of several BVs in NGC 6231 had uniquely peculiar spectra, *unlike any others seen before or since*. The low resolution *IUE* spectra of these stars have abnormally strong C IV$\lambda\lambda$1550 absorption. They also obtained an *IUE* high dispersion spectrum of the B1 V star, CPD-41°7719. Later, another high dispersion spectrum of the B0.5 V star, CPD-41°7724, was also obtained. The spectra of these stars are compared to the normal B0.5 IV star, λ Lep, in Figure 1. Because λ Lep was used as a flux standard by the *IUE* project, the spectrum shown is a mean of 78 spectra. All of the spectra were binned to 0.15 Å. Because λ Lep is a slow rotator, $v \sin i = 25$ km s^{-1} (Abt et al. 2002), it was necessary to broaden its spectrum to obtain good matches to the NGC 6231 stars. The λ Lep spectrum was convolved with a rotational broadening function (e.g., Gray 1976) of 50 km s^{-1} to match CPD-41°7719 and 90 km s^{-1} to match CPD-41°7724. The spectra were also shifted in radial velocity to align the Si III 1300Å triplets. The agreement of the important Si III 1300Å triplets and the 1417Å singlet, which are sensitive to the stellar parameters (Massa 1989), shows that λ Lep is a good spectral match for both stars, given the relatively poor S/N of the NGC 6231 spectra.

The one obvious difference between the NGC 6231 BVs and λ Lep is the high velocity C IV absorption trough in the NGC 6231 stars, which extends to ~ -2100 km s^{-1}. In addition, there is no hint of excess emission near $v \sim 0$, as one would expect from a normal wind. These profiles are very different from any seen in OB stars of any kind.[1] Massa et al. (1984) interpreted the peculiar absorption in terms of an abnormal wind. They were able to achieve a good fit to the high resolution profile but, in doing so, it was necessary to stretch the bounds of credibility. in order to model . Modeling profiles that show very strong high speed blue absorption with virtually no red emission with a spherically symmetric wind requires a wind that accelerates extremely rapidly, so that nearly all of the wind material capable of producing low speed emission is hidden behind the star. Further, this explanation is only plausible if one assumes that carbon is overabundant in the BVs. However, later analysis showed that the NGC 6231 BVs have fairly normal C abundance (e.g., Kilian et al. 1994).

This study included 4 BVs Massa et al. (1984) identified as peculiar (including CPD-41°7719), and all were found to have normal C abundances. In addition, over the years since Massa et al. (1984), no other examples of BVs with similar profiles have emerged (see, Walborn 1995). As a result, *an alternative explanation is needed.*

This paper proposes that the high speed absorption in the BVs actually results because they are immersed in a radially expanding flow originating elsewhere. Figure 2 shows the stars in the central region of NGC 6231. These are the stars listed in Table 4 of Baume et al. (1999) and CPD-41°7719, and includes 10 O stars, a B supergiant and WR 79. The symbol sizes are proportional to the V magnitudes and the coordinate system is in arcmin centered on WR 79. The red points indicate the positions of BVs observed in low dispersion by *IUE*. This includes the BVs HD 326328, HD 326332, HD 326333, CPD-41°7715, and Cl* NGC 6231 SBL, which were observed after the data used by Massa et al. (1984). Of these, the spectra of CPD-41°7715 and Cl* NGC 6231 SBL are peculiar by the Massa et al. (1984) criteria. Filled red points are BVs whose low dispersion spectra have peculiar C IV absorption, and open red points are BVs with normal spectra. The stars labeled 1 and 2 are CPD-41°7719 and CPD-41°7724, respectively, which have been observed in high dispersion by *IUE*. It is important to notice that *the stars with peculiar spectra are those closest to WR 79.*

It is emphasized that such peculiar absorption can only be observed in BVs for two reasons. First, they are strong UV sources at 1540 – 1550Å, so the absorption can be detected. Second, unlike more luminous B stars and O stars, they do not have strong, high speed absorption from their own winds, so it is possible to identify absorption due to a neighboring source.

3 TOTAL COLUMN THROUGH THE WIND

This section develops a simple model to help understand why it is so unusual to observe the absorption due to a stellar or cluster wind in background stars at great distances from the wind source, and why it is possible to see such a wind in the case of NGC 6231.

To begin, consider the absorption caused by a spherically symmetric wind when viewed by a second star within the far wind (termed the embedded star), which has no wind (or a very weak one), so that it can be used as a probe of the strong wind. Figure 3 shows the coordinate frame where the star with a massive wind is positioned at the origin and the embedded star is located at (x_1, y_1, z_1) and the observer is at $z = \infty$. The position of the star is labeled by (p_1, z_1), where p_1 is the impact parameter, defined as $p = (x^2 + y^2)^{1/2}$, so that the radial distance between the source and the embedded star is $r = (z^2 + p^2)^{1/2}$.

The region of interest is far from the source, where the wind has reached its terminal velocity, v_∞. Therefore, the wind density at z is $\rho(z) = \dot{M}/[4\pi v_\infty (z^2 + p^2)]$. The total column density of an absorbing ion through the wind to the embedded star is

$$N_{Tot} = \int_{z_1}^{\infty} \frac{\rho(z)}{\mu m_H} A_E q_i(z) dz = \frac{\dot{M} A_E q_i}{4\pi \mu m_H v_\infty p} \left(\frac{\pi}{2} - \tan^{-1} \frac{z_1}{p} \right) \quad (1)$$

where μ is the mean molecular weight of the gas, A_E is the atomic abundance of the absorbing element, $q_i(z)$ is the fraction of the element in ionization state i at the location z, and $q_i(z)$ was assumed to be constant in performing the integration. Inserting numerical values gives

$$N_{Tot} = \frac{9.74 \times 10^{15} \dot{M}_{-6} A_E q_i}{v_3 \mu p_{pc}} \left(\frac{\pi}{2} - \tan^{-1} \frac{z_1}{p} \right) \text{ cm}^{-2} \quad (2)$$

where $\dot{M}_{-6}$ is the mass loss rate in units of 10^{-6} $M_\odot$ yr^{-1},

[1] Disk winds are also capable of creating absorption with little accompanying emission. However, these winds are typically characterized by dense, low speed flows near the star (e.g., Bjorkman et al. 1994), and never show high speed absorption without strong low speed absorption. Thus, it is the presence of high speed absorption together with a lack of emission *and* low speed absorption, that make the profiles of the NGC 6231 BVs unique.

v_3 is the terminal velocity of the gas in thousands of km s^{-1}, and p_{pc} is the impact parameter of the line of sight in parsecs. This quantity enters the well known relation for equivalent width, $W_\lambda/\lambda_0 = 8.85 \times 10^{-21} \lambda_A f N_{Tot}$ (e.g., Spitzer 1978), where λ_0 is the rest wavelength of the transition and $\lambda_A f$ is the same wavelength in Å times the oscillator strength of the transition.

The following analysis concentrates on the C IV $\lambda\lambda$1550 doublet. For simplicity, this is treated as a single line with a combined $\lambda_A f = 442.692$, even though the wavelength ranges of the two components do not completely overlap. With these values the equivalent width in Å is

$$W_\lambda = 59.1 \frac{\dot{M}_{-6} A_E q_i}{v_3 \mu p_{pc}} \left(\frac{\pi}{2} - \tan^{-1} \frac{z_1}{p} \right) \quad (3)$$

Thus, the absorption seen by an embedded star with $p_{pc} = 1$ and $z_1 = 0$ (as reference values), due to an O star with a very massive wind ($\dot{M}_{-6} = 10$, $v_3 \simeq 2 - 3$), solar metalicity ($A_E = 3 \times 10^{-4}$ and $\mu \simeq 1.3$) and the extreme case where all of its carbon in C IV (i.e., $q_i \simeq 1$), would only be $\sim 45 - 68$ mÅ. Further, this absorption would be distributed over $10 - 15$ Å, making it impossible to detect. It would even be extremely difficult to measure absorption from a wind 10 times this strong. However, the situation is very different for WR 79. Because it is a WC star, its wind is carbon rich, with $A_E \gtrsim 0.1$ (e.g., Dessart et al. 2000). As a result, a WC star composed of 90% He and 10% C ($\mu \sim 4.3$), with $q_i \simeq 1$ and $\dot{M}_{-6} \simeq 10$ gives $W_A = 4.6 - 6.9$ Å, which is easily observed. Thus *the C IV equivalent width due to the wind of one WC star is stronger than one caused by more than 100 O stars with the same $\dot{M}$!*

4 MODEL PROFILES

For a spherically expanding wind, $\rho = \dot{M}/(4\pi r^2 v)$. Along a sight line with impact parameter p, this becomes $\dot{M}/[4\pi v_\infty (p^2 + z^2)]$, where we assume that p is very much larger than the stellar radius so that $v = v_\infty$ everywhere along the line of sight. However, what is measured is not z, but the line of sight velocity, v_z. From Figure 3, it is clear that $v_z(z) = v_\infty z/(z^2+p^2)^{1/2}$, where $v_z = c(\lambda - \lambda_0)/\lambda_0$, and λ_0 is the rest wavelength of the line in question. The expression for v_z can be inverted to obtain $z(v_z) = v_z p/(v_\infty^2 - v_z^2)^{1/2}$, and $\frac{dz}{dv_z} = v_\infty^2 p/(v_\infty^2 - v_z^2)^{3/2}$. Now, the total column density to a point z in the flow is $\int \rho(z) dz$, but this is needed in terms of v_z, i.e., $\rho(v_z)_{v_z}$, which is the total column density at v_z. Because $\int \rho(z) dz = \int \rho(v_z) \frac{dz}{dv_z} dv_z$, one has $\rho(v_z)_{v_z} = \rho(v_z) \frac{dz}{dv_z}$ for the density at v_z. Using the expressions for $z(v_z)$ and $\frac{dz}{dv_z}$ from above, one gets $\rho(v_z) = \dot{M}(v_\infty^2 - v_z^2)/(4\pi v_\infty^3 p^2)$ and

$$\rho(v_z)_{v_z} = \frac{\dot{M}}{4\pi v_\infty p (v_\infty^2 - v_z^2)^{1/2}} \quad (4)$$

This is converted to $N(v_z)_{v_z}$, the number of absorbing ions as a function of line of sight velocity,

$$N(v_z)_{v_z} = \frac{9.74 \times 10^{15} \dot{M}_{-6} A_E q_i(v_z)}{\mu v_3 p_{pc} (v_\infty^2 - v_z^2)^{1/2}} \text{ cm}^{-2} \text{ (km s}^{-1})^{-1} \quad (5)$$

for $v_1 \le v_z \le v_\infty$, where v_1 is the velocity at z_1. Notice that because the wind extends to $z = \pm\infty$, there is always a mathematical singularity at $v = -v_\infty$, and, if $z_1 = -\infty$, there will be another at $v = v_\infty$. To accommodate turbulent velocities along the line of sight, $N(v_z)_{v_z}$ is convolved with a normalized Gaussian turbulent velocity profile, $\phi(v_t : v_z)$, where v_t is the usual Gaussian b value, i.e., $\phi(v_t : v_z) \sim \exp -[(v - v_z)/v_t]^2$. This gives the optical depth as a function of velocity

$$\begin{aligned} \tau(v_z) &= \frac{\lambda_0 f}{\frac{m_e c}{\pi e^2}} N(v_z)_{v_z} \star \phi(v_t : v_z) \\ &= \frac{25.8 \lambda_0 f \dot{M}_{-6} A_E}{\mu p_{pc} v_3} \left[\frac{q_i(v_z)}{(v_\infty^2 - v_z^2)^{1/2}} \star \phi(v_t : v_z) \right] \end{aligned} \quad (6)$$

The resulting optical depths of the blue and red components, $\tau_b(v_z)$ and $\tau_r(v_z)$, are then shifted onto a common velocity scale and superimposed to produce the total optical depth of the doublet. Finally, a simple change of variables and exponentiation gives the residual intensity as a function of wavelength,

$$r(\lambda) = e^{-[\tau_b(\lambda) + \tau_r(\lambda)]} \quad (7)$$

which is equivalent to the transmission function of the wind.

Figure 4 shows examples of $r(\lambda)$ for constant $q_i(v_z)$. It demonstrates how the profiles respond to different values of v_1 and v_t. Note that for the wind of an isolated star, turbulent velocities $\sim 0.05 - 0.10 v_\infty$ are typically invoked. Given the chaotic nature of the intra-cluster environment and the colliding winds of the WR 79 binary, even larger values are not unreasonable.

5 FITS TO THE DATA

In this section, the *IUE* high resolution spectra of CPD-41°7719 and CPD-41°7724 are fit to the model developed in § 4. The ionization was assumed constant for the fitting procedure, i.e., $q_i(v_z) \equiv q_i$. This was necessary since its functional form is unknown and would be difficult to disentangle from the velocity parameters which determine the shape of the profile with the limited data available.

Four parameters are used in the fits. Three are velocity parameters: v_∞, the terminal velocity of the absorbing wind; v_t, the turbulent velocity of the wind, and; v_1, the wind velocity at the location of the embedded star. These 3 parameters determine the shape of the absorption profile. The fourth parameter, u_0, determines the strength of the absorption and is given by

$$u_0 = \frac{A_E \dot{M}_{-6} q_i}{\mu p_{pc}} \quad (8)$$

which has units of $10^{-6} M_\odot$ yr^{-1} pc^{-1}.

In addition to the absorption profile, a template is needed for the unabsorbed flux from the BV. As shown in Figure 1, the B0.5 IV star λ Lep is a good match to both stars, and even the low velocity portion of the C IV doublets are in reasonable agreement. Consequently, λ Lep was used as a template for both stars.

Although NGC 6231 has a large number of β Cep stars (e.g., Meingast et al. 2013), neither of the program stars have been identified as such. However, during 1996, *HST* GHRS G140L spectra were obtained for CPD-41°7719 during 3 consecutive orbits (spanning roughly 4 hours). Figure 5 compares the three GHRS spectra with the *IUE* high dispersion

spectrum degraded to the GHRS G140L spectral resolution of 135 km s^{-1}. Variability is clearly present in C IV, and most likely Si IV as well. However, the level is much smaller than typically observed in β Cep stars. This may indicate that CPD−41°7719 is a very low amplitude β Cep, perhaps with such a small optical amplitude that it has escaped detection in ground based searches. In any case, Figure 5 demonstrates that exact agreement with the low velocity portion of C IV, cannot be expected.

Figure 6 shows non-linear least squares fits to CPD−41°7719 and CPD−41°7724 by the absorption model using λ Lep as the underlying photosphere. The fits used the *IUE* errors for the normalized fluxes and the points crossed out are contaminated by low velocity interstellar C IV absorption along the line of sight. A single v_∞ was used for both fits. For a given fixed value of v_∞, the values of v_t, v_1 and u_0 were determined by a Levenberg Marquardt non-linear least squares routine. The best fit value of v_∞ was determined by a simple grid search. In both cases, χ^2 was a minimum for $v_\infty \simeq 1900 \pm 100$ km s^{-1}. The parameters derived from the fits are listed in Table 1 along with their 1σ errors. Considering the data quality data and the simplicity of the model, the fits are considered quite good.

The v_1 parameter can be used to infer the z_1 distance for each star. Assuming a spherical wind from WR 79, and letting α be the angle between the line of sight and the flow at z_1, one has $v_1 = v_\infty \cos\alpha$ and $p_1 = z_1 \tan\alpha$, so $z_1 = p_1 \cot[\cos^{-1}(v_1/v_\infty)]$. Using $d = 1.64$ kpc to convert the Table 1 data from arcmin to parsecs, results in $p_1 = 1.3$ and $z_1 = 2.20$ pc for CPD−41°7719 and 1.1 and 2.23 pc for CPD−41°7724.

Table 1 also lists the resulting W_λ values and their errors, which were calculated using the standard propagation of errors equation with numerical derivatives for the free parameters of the fit. Using equation (3), and the values of z_1 derived above, these can be rescaled to $z_1 = 0$ and $p_{pc} = 1$. The results are 7.66 and 7.61 Å for CPD−41°7719 and CPD−41°7724, respectively, which are close to the expectations given in § 3 for $q_i\ \dot{M}_{-6} \simeq 10$.

6 DISCUSSION

This discussion examines the evidence favoring the proposed interpretation of the C IV absorption seen in the BVs and describes how the model could be used to constrain the kinematics of the flow if more data were available.

To assess the validity of the model, both direct and indirect evidence is examined. Beginning with the direct information, I compare the fit parameters (v_∞, v_t, v_1, u_0) given in Table 1 to known quantities and processes relevant to WR stars and H II regions. The best fit v_∞ (1900 km s^{-1}) differs by only 16% from 2270 km s^{-1}, the v_∞ determined for WR 79 by Prinja et al. (1990). The large errors for v_t show that they are poorly constrained by the data. Nevertheless, values of 300 km s^{-1} are common for WC stars (e.g., Hillier 1989), so considering the large errors and the chaotic nature of the NGC 6231 environment due to the presence of several O stars, the derived values for v_t are considered reasonable. While v_1 is not directly measurable, it was shown in the previous section that it can be used to derive the distance from the star to the wind source. It was found that $z_1 = 2.20$ and 2.23 pc for CPD−41°7719 and CPD−41°7724, respectively. These values are only about twice their impact parameters and, therefore, consistent with the observed size of the cluster. They also indicate that the 2 BVs are in front of WR 79. Combining the z_1 and impact parameters gives the radial distance of each star from WR 79. These are 2.57 and 2.46 pc for CPD−41°7719 and CPD−41°7724, respectively.

Knowing that the BVs are 2 pc or more from WR 79, it is possible to estimate two important properties about the gas along their lines of sight. First, it takes the absorbing gas ~ 1000 yrs to travel from the stellar surface to the where it begins to absorb. Second, The mean number density of the wind 2 pc from the star is $0.0032\ M_{-6}/(\mu r_{pc} v_3) \simeq 1.57 \times 10^{-4}\ M_{-6}$ cm^{-3}. Thus, the absorbing material exists in a very rarefied environment.

The parameter u_0, given by equation (8), is composed of quantities that can be constrained by measurements and q_i, which cannot. Consequently, the process is turned around. A value for u_0 is adopted and then it is determined whether reasonable values of q_i result. To begin, equation (8) is solved for q_i

$$q_i = u_0 p_{pc} \left(\frac{\mu}{A_E}\right) \frac{1}{\dot{M}_{-6}} \tag{9}$$

Values for u_0 and p_{pc} are set to their means from Table 1, 1.2 pc and 0.31 $10^{-6} M_\odot$ yr^{-1} pc^{-1}, respectively. The ratio μ/A_E depends on the chemical composition or the WR 79. If it composed of helium and carbon with $0.08 \le A_E \le 0.25$ (Dessart et al. 2000), it will have $4.23 \le \mu \le 4.80$ and $0.02 \le A_E/\mu \le 0.05$. Previous estimates for $\dot{M}$ of WR 79 are 2.8×10^{-5} M$_\odot$ yr^{-1} from its photometric light curve (Lamontagne et al. 1996) and 9×10^{-5} M$_\odot$ yr^{-1} from its radio fluxes (Willis 1991). Clearly, q_i must be less than one. The smallest possible value of q_i consistent with the data is determined by using the smallest value for μ/A_E and the largest for $\dot{M}_{-6}$. This gives $q_i \simeq 0.08$. Therefore, for the model to be consistent, q_i must be $\gtrsim 0.08$. Unfortunately, wind models offer little information about q_i at such large distances from the star, since they rarely extend beyond ~ 100 stellar radii. However, most models do predict that the outer wind cools to $\sim$ 10kK (e.g., Hillier 1989; Nugis et al. 1998), and that nearly all of the C is in C III. However, the wind material almost certainly contains optically thick clumps (e.g., Aldoretta et al. 2016, and references therein), and at such great distances from the star, it must co-exist with the radiation field from the cluster O stars and the X-ray emitting gas in the cluster (Sana et al. 2007). These effects are not considered in WR wind models. As a result, q_i for C IV is difficult to predict without a better understanding of the structure of the flow and detailed modeling, which are far beyond the scope of the current paper. Nevertheless, some guidance can be gleaned from interstellar calculations. First, note that C IV is a well known tracer of highly ionized gas in H II regions where, for low density environments, $q_i \sim 1$ (de Kool & de Jong 1985). Second, C IV is also an indicator of cooling gas in the temperature range of 80 to 150 kK (e.g., Sutherland & Dopita 1993) where $q_i \sim 0.1$. These conditions are found at interfaces between million degree gas and denser clumps (e.g., Savage & Wakker 2009) – similar to the conditions in a clumped wind, described above. Consequently, it seems quite plausible that $0.1 \lesssim q_i \lesssim 1.0$, depending on ex-

actly how the wind is structured and the influence of the surrounding conditions.

It is also possible that the absorption is not due to just the wind of WR 79, but a collective wind whose carbon abundance has been enhanced by WR 79. To address this issue, consider the contributions to the wind flow of the 10 O stars (11 when both components of HD 152248 are included) and one B supergiant shown in Figure 2. Their mass loss rates were estimated by beginning with the spectral types given by Baume et al. (1999). These were translated to physical parameters using the Martins et al. (2005) calibration for Galactic O stars (as modified by Weidner & Vink 2010) which were then used to determine mass loss rates through the Vink et al. (2000) relations. The combined $\dot{M}$ for all of these stars is 1.2×10^{-5} $M_\odot$ yr^{-1}. While these winds contribute very little to the C IV absorption, they could influence the wind flow from WR 79. The two components of the binary HD 152248 account for roughly half of the O star contribution. Together, their mass loss is expected to be $6.1{\times}10^{-6}$ $M_\odot$ yr^{-1}. Further, the system is much closer (on the sky) to the two BVs (it is the bright star that touches CPD-41° 7724 in Figure 2). So although its wind should contribute little to the C IV absorption, its momentum could have a strong influence on the flow that is traced by the C IV from WR 79, possibly channeling it toward the line of sight to the cluster and affecting the ionization. Unfortunately, given the few sight lines available, it is currently not possible to pursue this possibility further.

In terms of indirect support for the current model, consider the statement made in § 2 that BVs with anomalous spectra like those in NGC 6231 have not been observed before or since in more detail. Specifically, beginning with the WC stars listed in the van der Hucht (2001) catalog with $V \leq 9$ mag, the *IUE* archive was searched for BVs (with an SWP spectrum of any kind) within 30 arcmin of each. WR 79 is the only WC near BVs. There is a reason for this. Normal, faint BVs were not typically observed with *IUE*. Normal BVs are 2 to 4 mags fainter than O, B supergiant or WR stars. Consequently, there was very little motivation to observe them, when bright nearby BVs were available. However, one reason to observe faint BVs in open clusters was to use them as standard candles for extinction studies – which is how the BVs with peculiar spectra in NGC 6231 were uncovered. These extinction studies observed numerous BVs in several young, open clusters (e.g., Fig. 1 in Fitzpatrick & Massa 2007), but only NGC 6231 contained a WC star *and* only NGC 6231 contained BVs with peculiar spectra. Since it is now known that the NGC 6231 BVs have normal abundances (Kilian et al. 1994), the only thing that makes them unique is that they cohabit a cluster with a WC star.

To summarize, it was argued that the high speed C IV absorption is probably not intrinsic to the NGC 6231 BVs but related to the wind of WR 79 for the following reasons:

(i) The BVs in NGC 6231 have normal abundances, so there is no reason to expect their winds to be abnormal.

(ii) Of the BVs observed in young clusters with *IUE*, only NGC 6231 contains BVs with peculiar C IV absorption, *and* only NGC 6231 contains a WC star.

(iii) The NGC 6231 BVs with peculiar C IV are located near WR 79, and those further away have normal spectra (§ 2).

(iv) The BV absorption profiles are well modeled by the profiles expected for stars embedded in a spherically expanding flow.

(v) The values of v_∞, v_1, $\dot{M}_{-6}$, A_E and q_i determined from the profile fits all lie within the range of expected values.

While not conclusive, these facts imply that it is highly probable that WR 79 is responsible for the high speed absorption. Unfortunately, the available data do not make it possible to determine whether the flow is dominated by the wind of WR 79, or simply enriched in carbon by it. This is because the two available lines of sight are close together and roughly the same distance from WR 79. As a result, they do not provide much independent information for distinguishing whether the high speed gas is coming from WR 79 or a more extended source. Only additional sight lines with different locations in the cluster can brake this degeneracy.

ACKNOWLEDGEMENTS

This paper benefited from the comments of an anonymous referee, and discussions with W.-R. Hamann and L. Oskinova. D.M. acknowledges partial support under NASA Grants NNX11AB19G and HST GO-13760 to SSI. The data presented in this paper were obtained from the Mikulski Archive for Space Telescopes (MAST). STScI is operated by the AURA, Inc., under NASA contract NAS5-26555. Support for MAST for non-HST data is provided by the NASA Office of Space Science via grant NNX09AF08G and by other grants and contracts. The DSS2 was produced at the STScI, under grant NAG W-2166.

REFERENCES

Abt, H. A., Levato, H. & Grosso, M. ApJ, 2002, 573, 359
Aldoretta, E.J., St-Louis, N., Richardson, N.D., Moffat, A.F.J. et al. 2016, MNRAS, 460, 3407
Balona, L. A. & Laney, C. D. 1995, MNRAS, 276, 627
Baume, G., VÃązquez, R.A. & Feinstein, A. 1999 A&AS, 137, 233
Bjorkman, J.E., Ignace, R., Tripp, T.,M. & Cassinelli, J.P. 1994, ApJ, 435, 416
Cappa, C.E., Goss, W.M. & Pineault, S. 2002, AJ, 123, 3348
Cazzolato, F. & Pineault, S. 2000, AJ, 120, 3192
de Kool, M. & de Jong, T. 1985, A&A, 149, 151
Dessart, L., Crowther, P.A., Hillier, D.J., Willis, A.J., Morris, P.W. & van der Hucht, K.A. 2000, MNRAS, 315, 407
Feinstein, C., Martnez, R., Vergne, M.M., Baume, G. & VÃązquez, R. 2003, ApJ, 598, 349
Fitzpatrick, E. L. & Massa, D. 2007, ApJ, 663, 320
Gray, D.F. 1976, The observation and analysis of stellar photospheres, New York, Wiley-Interscience
Hill, G.M., Moffat, A.F.J., St-Louis, N. & Bartzakos, P. 2000, MNRAS, 318, 402
Hillier, D.J. 1989, ApJ, 347, 392
Kilian, J., Montenbruck, O. & Nissen, P.E. 1994, A&A, 284, 437
Lamontagne, R., Moffat, A.F.J., Drissen, L., Robert, C. & Matthews, J.M. 1996, AJ, 112, 2227
Martins, F., Schaerer, D. & Hillier, D.J. 2005 A&A, 436, 1049
Massa, D., Savage, B. D., & Cassinelli, J. P. 1984, ApJ, 287, 814
Massa, D. 1989, A&A, 224, 131
Meingast, S., Handler, G. & Shobbrook, R.R. 2013 A&A, 559, A108

Nazé, Y., Rauw, G., Manfroid, J., Chu, Y.-H. & Vreux, J.-M. 2003, A&A, 408, 171
Nugis, T., Crowther, P.A. & Willis, A.J. 1998, A&A, 333, 956
Prinja, R. K., Barlow, M.J. & Howarth, I.D. 1990, ApJ, 361, 607
Sana, H., Rauw, G., Sung, H., Gosset, E. & Vreux, J.-M. 2007, MNRAS, 377, 945
Sander, A., Hamann, W.-R. & Todt, H. 2012, A&A, 540, A144
Savage, B.D. & Wakker, B.P. 2009, ApJ, 702, 1472
Schild, R.E., Hiltner, W.A. & Sanduleak, N. 1969, ApJ, 156, 609
Spitzer, L. 1978, "Physical processes in the interstellar medium", New York Wiley-Interscience.
Sutherland, R.S. & Dopita, M.A. 1993, ApJS, 88, 253
Tuthill, P.G., Monnier, J.D., Lawrance, N., Danchi, W.C., Owocki, S.P. & Gayley, K.G. 2008, ApJ, 675, 698
van der Hucht, K.A. 2001, New Astron. Rev., 45, 135
Vink, J.S., de Koter, A. & Lamers, H.J.G.L.M. 2000, A&A, 362, 295
Walborn, N.R., Parker, J.W. & Nichols, J.S. 1995, International Ultraviolet Explorer Atlas of B-type spectra from 1200 to 1900 Å, NASA Reference Publication, 1363
Weidner, C. & Vink, J.S. 2010, A&A, 524, A98
Willis, A.J. 1991, in van der Hucht K.A., Hidayat B., eds, IAU Symposium Vol. 143, Wolf-Rayet Stars and Interrelations with Other Massive Stars in Galaxies, p. 265

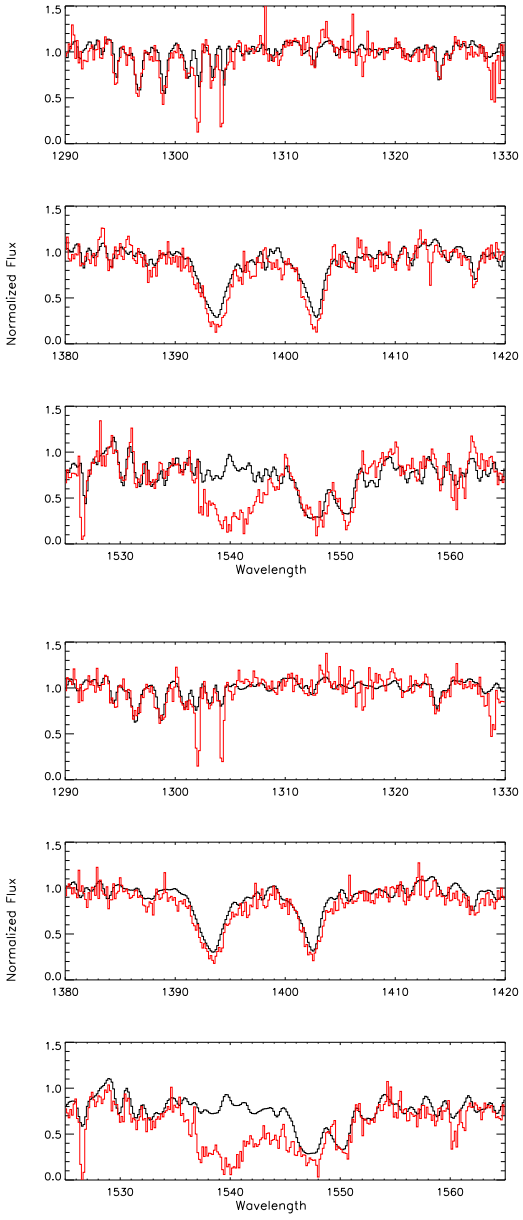

Figure 1. Comparisons of the NGC 6231 BV spectra (red) with that of the normal B0.5 IV star λ Lep (black). Top three panels: λ Lep and CPD−41°7719 (B1 V). Bottom three panels: λ Lep and CPD−41°7724 (B0.5 V). All spectra are binned to 0.15 Å. Aside from the stronger interstellar spectrum and the pronounced high velocity C IV absorption in the NGC 6231 stars, the agreement with λ Lep is very good.

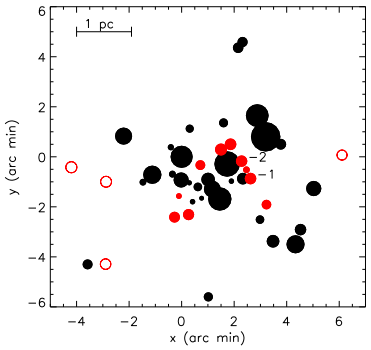

Figure 2. Stars in the central region of NGC 6231. This includes the stars listed in Table 4 of Baume et al. (1999) and CPD−41°7719. The size of 1 pc is shown for a distance of 1.64 kpc. The symbol sizes are proportional to V magnitudes and the coordinate system is centered on WR 79. Red points represent BVs observed by *IUE*. Filled red points are for stars whose low dispersion spectra contain C IV peculiarities, and open red points are for stars with normal spectra. The stars labeled 1 and 2 are CPD−41°7719 and CPD−41°7724, respectively, which were observed at high resolution with *IUE*.

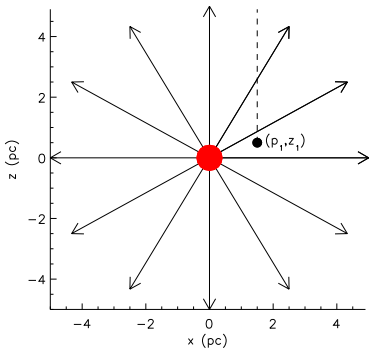

Figure 3. Schematic of a wind emerging from a star at the origin and a star embedded in the wind. The embedded star is located at (x_1, y_1, z_1) and labeled by (p_1, z_1), where $p = (x^2 + y^2)^{1/2}$ is the impact parameter. The dashed line points to the observer. It is clear that the range of velocities which absorb along the line of sight is dictated by the position of the star in the wind.

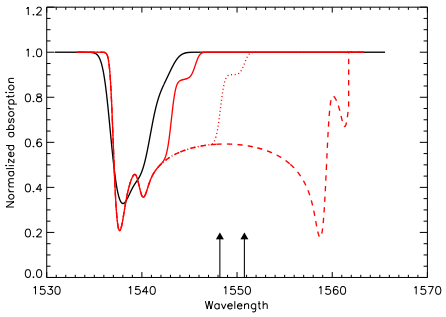

Figure 4. A set of model profiles of the C IV absorption expected for embedded stars. All of profiles have $v_\infty = 2100$ km s^{-1} and the arrows indicate the rest wavelengths of the C IV doublet. The black profile has a turbulent velocity of 200 km s^{-1} and $v_1 = -1500$ km s^{-1}, implying that the embedded star is well in front of the wind source. The red profiles have a turbulent velocity of 100 km s^{-1} and $v_1 = -1000$ km s^{-1}(solid), 0 km s^{-1}(dotted) and +2100 km s^{-1}(dashed). The profiles with $v_1 = 0$ and +2100 km s^{-1} show how broad, featureless absorption can be present and that even red absorption can exist in stars well beyond the wind source.

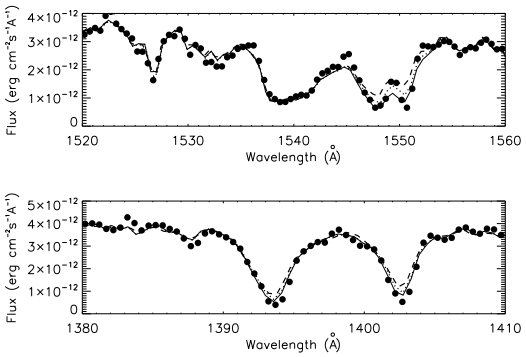

Figure 5. Comparison of 3 GHRS G140L spectra of CPD−41°7719 (solid, dashed and dotted curves) taken on consecutive orbits and an *IUE* high resolution spectrum binned to the GHRS G140L resolution (points).

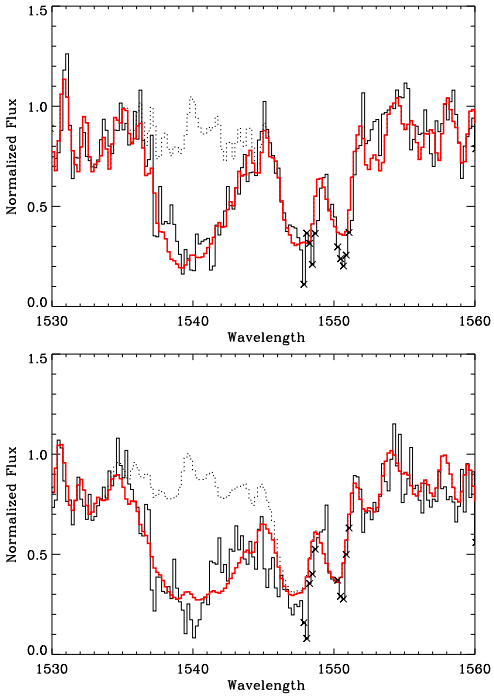

Figure 6. Fits to CPD−41°7719 (left) and CPD−41°7724 (right) using the parameters listed in Table 1. The black spectra are the observed spectra, and the crosses represent points excluded from the fits due to interstellar contamination. The dotted spectrum is λ Lep (which was used as a template for both stars), and the red spectra are the fits, which are the dotted spectrum multiplied by the model absorption profile.

Table 1. Fit parameters

Star	Sp Ty	p_1 arcmin	v_∞ km s^{-1}	v_t km s^{-1}	v_1 km s^{-1}	u_0 $10^{-6} M_\odot$ yr^{-1} pc^{-1}	W_λ Å
CPD−41°7719	B1 V	2.8	1900 ± 100	310 ± 83	1319 ± 130	0.32 ± 0.05	4.25 ± 0.57
CPD−41°7724	B0.5 V	2.3	1900 ± 100	507 ± 105	1021 ± 78	0.31 ± 0.05	5.37 ± 0.58

This paper has been typeset from a TEX/LATEX file prepared by the author.